SAND97-0480C
CONF-970344--2

3D ELECTROMAGNETIC INVERSION FOR ENVIRONMENTAL SITE CHARACTERIZATION

David L. Alumbaugh and Gregory A. Newman
Geophysics Department, MS 0750
Sandia National Laboratories
Albuquerque, NM 87185
Phone: (505)844-0555
EMail : dlalumb@sandia.gov

ABSTRACT

A 3-D non-linear electromagnetic inversion scheme has been developed to produce images of subsurface conductivity structure from electromagnetic geophysical data. The solution is obtained by successive linearized model updates where full forward modeling is employed at each iteration to compute model sensitivities and predicted data. Regularization is applied to the problem to provide stability. Because the inverse part of the problem requires the solution of 10's to 100's of thousands of unknowns, and because each inverse iteration requires many forward models to be computed, the code has been implemented on massively parallel computer platforms. The use of the inversion code to image environmental sites is demonstrated on a data set collected with the Apex Parametrics 'MaxMin I-8S' over a section of stacked barrels and metal filled boxes at the Idaho National Laboratory's 'Cold Test Pit'. The MaxMin is a loop-loop frequency domain system which operates from 440 Hz up to 56 kHz using various coil separations; for this survey coil separations of 15, 30 and 60 feet were employed. The out-of phase data are shown to be of very good quality while the in-phase are rather noisy due to slight mispositioning errors, which cause improper cancellation of the primary free space field in the receiver. Weighting the data appropriately by the estimated noise and applying the inversion scheme is demonstrated to better define the structure of the pit. In addition, comparisons are given for single coil separations and multiple separations to show the benefits of using multiple offset data.

INTRODUCTION

Frequency domain, controlled source electromagnetic methods are routinely employed to map the location of barrels, trenches and pits, metals, plumes, etc., at hazardous waste sites. Although the raw data provides excellent resolution regarding the horizontal location of these targets, it directly yields very little information about their vertical extent and often cannot define sharp boundaries. In order to produce high resolution images of the subsurface conductivity structure, non-linear inversion or approximate imaging techniques must be applied to the data. However, in areas where there are large contrasts in subsurface conductivity, the approximate techniques can often break down. Thus in order to produce high accuracy images in many areas, a non-linear inversion approach must be applied.

The full non-linear inversion problem has historically been hindered by insufficient computing resources. Even today, only the largest computers provide the computational speed and memory allocation necessary to successfully handle this problem. Thus here we employ a non-linear inversion scheme that runs on massively parallel computer platforms (Newman and Alumbaugh, 1997). The code incorporates a staggered finite difference scheme to accurately compute the model sensitivities and predicted data (Alumbaugh et al., 1995), and uses the method of conjugate gradients to solve the inverse portion of the problem. This method for handling large inverse problems has been employed by Zhang et al. (1995) to solve 3D direct current (DC) inverse problem, Mackie and Madden (1993) for

DISCLAIMER

3D magnetotelluric (MT) inversion, and Newman and Alumbaugh (1997) for the 3D controlled source EM inversion problem.

A second important factor that must be considered in order to produce highly accurate images of the subsurface is the quality and amount of data that are collected. Typically used frequency domain systems either collect multi-frequency data for a single source-receiver separation, or employ a single frequency for multiple separations. In this paper we use initial results from the 3-D inversion scheme to illustrate that much better estimates of subsurface structure are achieved when multiple frequency data are collected at multiple coil separations. The is due to the fact that data collected at smaller source-receiver separations are more sensitive to the near surface, while large separation data yield valuable information about the conductivity of deeper structures. This fact will be demonstrated with a set of data collected using the Apex Parametrics MaxMin I- 8S system over the Cold Test Pit at the Idaho National Engineering Laboratory in June of 1996. The data quality will be discussed, as well as the problems associated with performing such a survey and inverting the data.

THE INVERSE SOLUTION

Before describing the survey and the data, a brief description of the inversion scheme is given. For a more thorough description, the reader is referred to Newman and Alumbaugh (1997).

A key consideration in developing any inverse solution is the efficient computation of model sensitivities. Because we will solve the inverse problem from an underdetermined point of view, we can efficiently carry out calculations involving model sensitivities using reciprocity. The use of reciprocity, or the adjoint solution to Maxwell's equations where the receivers act as sources, limits the number of forward models that need to be computed to the number of the transmitter and unique receiver positions for a given frequency. In fact, using the adjoint approach coupled with the conjugate gradient solution to the inverse problem allows one to avoid even forming individual components of the model sensitivity matrix, hence resulting in additional computational savings (Zhang et al., 1995).

The parameterization used in the 3D inverse solution will be kept sufficiently fine because we are interested in reconstructions that do not under parameterize the earth. This forces the 3D inverse problem to be underdetermined, which makes it unstable and ill posed. Reliable estimates of the model parameters **m** may be possible if a least squares inversion is stabilized with regularization (Tikhonov and Arsenin, 1977). Regularization removes solutions that are too rough by imposing an additional constraint on the model. Reconstructions are required to be smoothed versions of the earth's electrical properties at the expense of an increase in the fitting error.

Linearizing about a given earth model, $\mathbf{m}^{(\mathbf{i})}$, at a given iteration **i**, the following functional can provide smooth reconstructions if it is minimized with respect to the desired model parameters, **m**, which in this case will be the electrical conductivity:

$$S = \left[\left(\mathbf{D}\left(\mathbf{d}-\mathbf{d}^{\mathbf{p(i)}}\right)-\mathbf{A}^{\mathbf{p(i)}}\left(\mathbf{m}-\mathbf{m}^{(\mathbf{i})}\right)\right)^{\mathbf{T}}\left(\mathbf{D}\left(\mathbf{d}-\mathbf{d}^{\mathbf{p(i)}}\right)-\mathbf{A}^{\mathbf{p(i)}}\left(\mathbf{m}-\mathbf{m}^{(\mathbf{i})}\right)\right)-\chi^2\right] + \lambda(\mathbf{Wm})(\mathbf{Wm})^{\mathbf{T}}. \quad (1)$$

The idea is to minimize model roughness, $(\mathbf{Wm})(\mathbf{Wm})^{\mathbf{T}}$ (the superscript **T** denotes the transpose operator) subject to an estimated data error (χ^2). The roughness or regularization matrix (**W**) consists of a finite difference approximation to the Laplacian (∇^2) operator

and is sparse, and λ is the tradeoff parameter between model roughness and data fit (a description of how λ is chosen is given below). Also in this equation, the observed data are represented by the vector **d,** and the predicted data arising from the model $\mathbf{m}^{(i)}$ at the i'th iteration of the inversion procedure are denoted by $\mathbf{d}^{\mathbf{p}(i)}$. These values are calculated using the finite differences scheme given in Alumbaugh et al. (1996). The data weighting matrix **D** is diagonal and consists of individual estimates of the data noise. The Jacobian or model sensitivities matrix is given by $\mathbf{A}^{\mathbf{p}(i)}$, and for arithmetic simplicity it is split into real and imaginary components such that the estimated model parameters are real. Determining and manipulating the elements of the Jacobian matrix in the most efficient manner is critical for a robust 3D inverse solution, since calculation and use of these elements can be a bottleneck in the inversion.

Minimization of equation (1) yields the model update, i.e.,

$$\mathbf{m} = \left[\left(\mathbf{DA}^{\mathbf{p}(i)}\right)^{\mathbf{T}}\left(\mathbf{DA}^{\mathbf{p}(i)}\right) + \lambda \mathbf{W}^{\mathbf{T}}\mathbf{W}\right]^{-1}\left(\mathbf{DA}^{\mathbf{p}(i)}\right)^{\mathbf{T}}\mathbf{D}\delta\mathbf{d}^{(i)} \qquad (2)$$

where

$$\delta\mathbf{d}^{(i)} = \mathbf{d} - \mathbf{d}^{\mathbf{p}(i)} + \mathbf{A}^{\mathbf{p}(i)}\mathbf{m}^{(i)}. \qquad (3)$$

However, because negative parameter estimates are an admissible solution arising from equation (2), it is advisable that before the minimizing equation (1) it should be reformulated to invert for the natural logarithm of the parameters rather than the parameters themselves. This enforces positivity constraints on the solution which is a physical requirement. In addition, by using the log parameterization it is also possible to incorporate a lower bound constraint on the inverse solution by setting

$$\mathbf{m} - \mathbf{m}^{(i)} = \left(\mathbf{m}^{(i)} - \varepsilon\right) ln\left(\left(\mathbf{m} - \varepsilon\right)/\left(\mathbf{m}^{(i)} - \varepsilon\right)\right). \qquad (4)$$

Again for more information on how this is done and/or how the resulting systems of equations is solved using the conjugate gradient method refer to Newman and Alumbaugh (1997).

The final consideration in the operation of the inverse scheme is how to choose λ as its selection requires special care if the solution is to provide acceptable results. Selecting tradeoff parameters that are too small can produce models that fit the data well but are physically unreasonable with rapid spatial variation. Selecting tradeoff parameters that are too large produce highly smoothed models which show poor dependence on the data. Thus we have chosen an approach where by for the first iteration λ is large enough to provide a reasonably smooth solution. It is then relaxed with progressive iterations as described below such that we gradually incorporate more resolution into the image.

The iterative procedure is initiated by assuming some initial background model, where we compute the predicted data and electric field for all transmitter and unique receiver locations. At the first iteration we calculate the model update via equation (2) with the appropriate selection of the tradeoff parameter to provide a smooth model. Although there are many ways of choosing λ (e.g. Constable, et al., 1987, Park and Van, 1991, Oldenburg, 1994), we have chosen to assign λ as

$$\lambda = \text{Max Row Sum}(\mathbf{DA}^{\mathbf{p}(i)}\,[\mathbf{DA}^{\mathbf{p}(i)}]^{\mathbf{T}})/2^{(i-1)}. \qquad (5)$$

With this selection, the tradeoff parameter estimates the largest eigenvalue or equivalently the amplifying power of the non-regularized least squares system matrix at the first iteration. At each subsequent iteration the smoothness parameter is chosen by reducing this amplifying power by a factor of $2^{(i-1)}$ where i is the present iteration number. This allows for fairly quick convergence which is a necessity for the size of problems under analysis, while providing the smoothness constraint to be gradually relaxed.

After the model update is determined, the predicted data for the are computed and the residual error between the predicted and measured data calculated. If the sum of the squared residual errors is less than χ^2, if this residual error level has converged to a value greater than χ^2, or if the number of iterations has obtained some predefined limit, the process is terminated. Otherwise the scheme proceeds to the next iteration where it linearizes about the new model **m**, computes the electric fields for the updated background model and determines the new model update with the tradeoff parameter specified by equation (5).

For 2-D problems, the above scheme will operate efficiently on today's high end computer workstations. However, for the 3-D case it is generally necessary to employ massively parallel computers due to the number of sources and receivers employed and the size of the forward modeling and inversion domains. Thus we have modified the original version of the code to operate on these types of platforms. However, because the description of this process is beyond the scope of this paper, we refer the readers to Alumbaugh et al. (1996) and Newman and Alumbaugh (1997) for information about how this parallelization process is incorporated.

DESCRIPTION OF THE GEOPHYSICAL SURVEY AND DATA

The data analyzed in this study were collected with the Apex Parametrics MaxMin I-8S frequency domain system (Apex Parametrics, 1994) at the Idaho National Engineering Laboratory's Cold Test Pit (CTP) as part of the DOE sponsored Electromagnetic Integrated Demonstration (EMID) project. For more information about the CTP, the reader is referred to a report by Lockheed Idaho Technologies Company (1994), while for more information about the EMID, see Pellerin et al. (1997, this volume).

The MaxMin I-8S system is a loop-loop frequency domain system consisting of a small transmitter loop (approximately 0.5m on a side) connected to a ferrite coil receiver system by a reference cable of various length. Coil separations of 15, 30 and 60 feet were employed during the survey using eight frequencies ranging from 440 Hz to 56320 Hz in bilinear steps. Both the transmitter and receiver units are worn by the operators using shoulder harnesses. The in-phase and out-of-phase components of the scattered magnetic field are measured in terms of percentage of the free space or primary field. The data are acquired by manually stepping through each frequency and dumping the result to the digital acquisition system, or MaxMin computer (MMC), which also records the station location as well as the standard deviation of the data and the tilt of the instruments. Basic data processing is accomplished using software provided by Apex Parametrics.

The system allows for four different coil configurations to be employed: a max1 configuration in which the windings for both the source and receiver are horizontal, a max2 configuration which uses vertically oriented windings, and two minimum coupled configurations in which the windings are orthogonal to each other. For this survey, the max1 configuration was used throughout.

The in-phase primary or free-space field produced by the transmitter is canceled at the receiver by "bleeding" current off of the transmitter to exactly oppose the current induced by this unwanted component in the receiver. This causes the measured in-phase

field to be very sensitive to errors in the source-receiver separation. For example, a change in positioning of one inch between the coils for a 60 foot separation produces an error of approximately 1% of the primary field. At smaller source-receiver separations this sensitivity to mispositioning is increased. Thus at each station the measurements were initialized at 440 Hz by crudely positioning the source and receiver using the CTP measurement grid (Pellerin et al.,1997, this volume), and then finely adjusting the position of either the source or receiver such that the receiver output indicated an in-phase reading that was as close to zero as possible. This usually resulted in a 440 Hz in-phase reading between ± 0.5% of the primary field. This was determined to be an applicable method for positioning because at this low frequency and these close coil separations the in-phase field should be very small, i.e., near the resolution of the unit. In addition, positioning in this manner had no effect on the out-of-phase reading. After positioning, the datum for each of the remaining frequencies was measured and entered into the computer before moving to the next station.

The survey was limited to the four primary lines of the CTP (See Figure 1 in Pellerin et al., 1997, this volume). For the 15 and 30 foot separations, data were sampled at five foot intervals along each of the lines. For the 60 foot separation a 10 foot sampling was employed for every line except the repeat line, which was sampled at 5 foot intervals along line 7.5N. The receiver unit was maintained at a height of approximately 4' 3" off the ground, while transmitter coil was 2' 7 1/4" off the ground.

The data have been plotted in gray-scale maps for each frequency in Figure 1 for the 60 foot source-receiver separation, and in Figure 2 for the 15 foot offset (the 30 foot offset data have not been displayed in order to conserve space). In general, these data show an anomaly over the center of the four lines corresponding to the buried barrels and boxes, especially at 60 feet offset. However, note that the in-phase component is much noisier spatially from one point to another than the out-of-phase, and that this noise increases with decreasing coil separation. In fact the in phase component of the field for the 15 foot offset resembles a random noise distribution. This is due to the in-phase sensitivity of the system to the source-receiver separation with regards to canceling the primary field. On the other hand, the out-of-phase data appears to be fairly stable and robust. Finally, notice that at the highest two frequencies for the 15 foot offset, the response of the target zone within the pit is almost unresolvable. This signifies that at these frequencies and source-receiver offset we are only sensing the capping material covering the pit.

A more robust analysis of the data quality was conducted by incorporating a repeat survey of line 7.5N using a 60 foot coil separation. As shown in Figure 3, the out-of-phase component repeats fairly well, generally within 0.2%. The in-phase component, however is not as reproducible. (Note, in this comparison the in-phase component at each station has had the value measured at 440 Hz subtracted off to remove the bias that is present.) This is due, once again, to the positioning sensitivity of the sensors to the unwanted primary field. This analysis, along with a general qualitative description of the data served as the basis for estimating the error (or noise) present in the data, as these errors were much larger than the standard deviations measured by the system during the survey. In general the estimated noise for the out-of-phase component ranged from 0.1% at the lower frequencies to 0.6% at the higher, while the in-phase noise was estimated to be 2% for all frequencies.

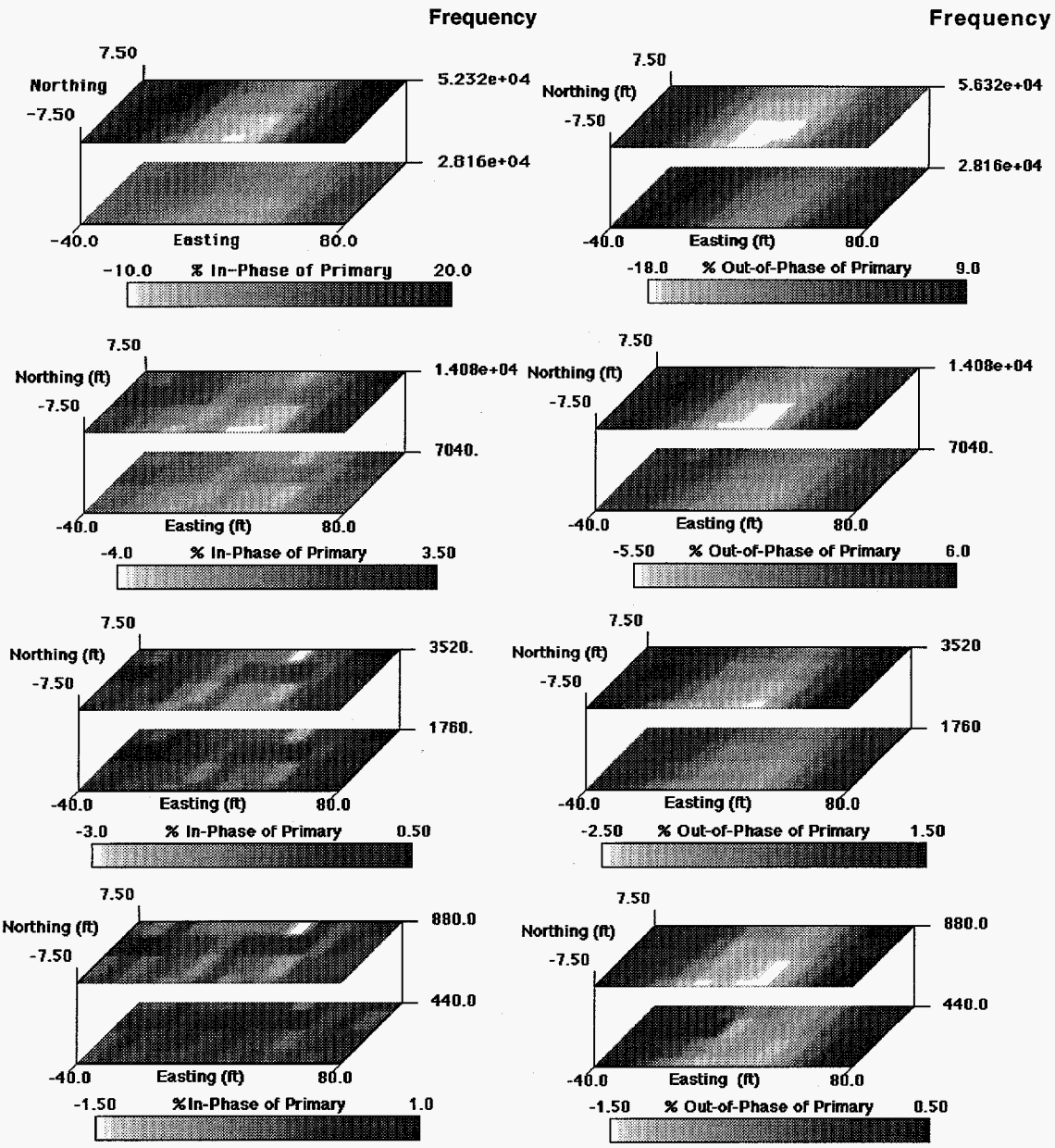

Figure 1 - Map plots of the data collected with the MaxMin I-8S system over the four primary lines of the CTP using a 60 foot coil separation. The in-phase components are on the left, and the out-of-phase on the right. The frequency data are displayed in four pairs of two to better demonstrate the dynamic range found in the measurements.

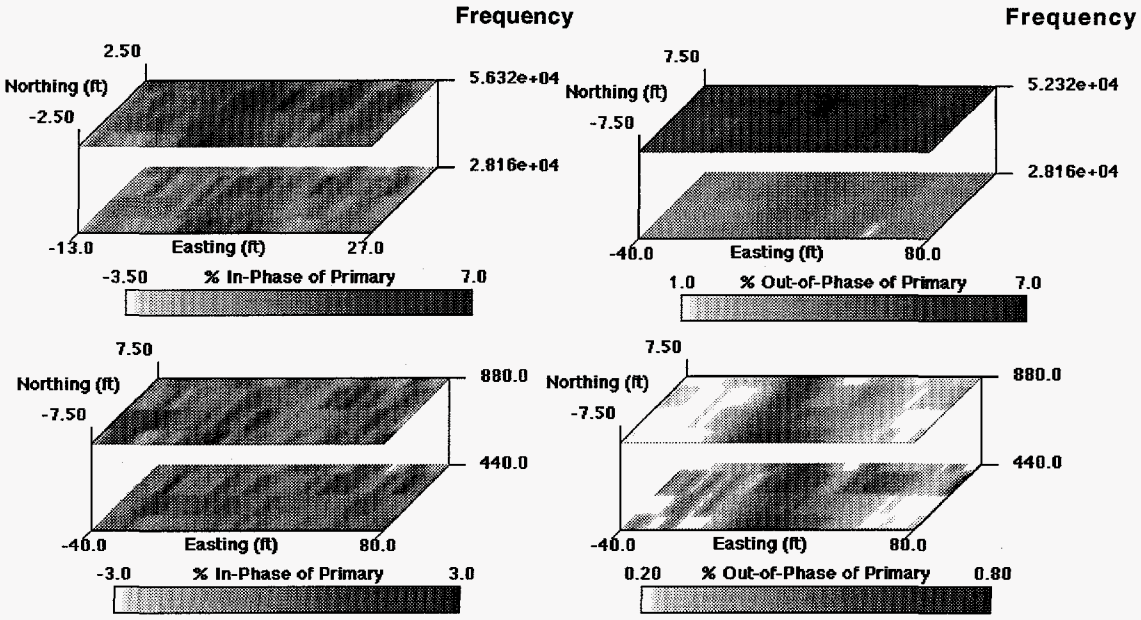

Figure 2 - Map plots of the data collected with the MaxMin I-8S system over the four primary lines of the CTP using a 15 foot coil separation. The in-phase components are on the left, and the out-of-phase on the right. The frequency data are displayed in two pairs of two to better demonstrate the dynamic range found in the measurements (we have included only the lowest and highest frequencies due to space limitations).

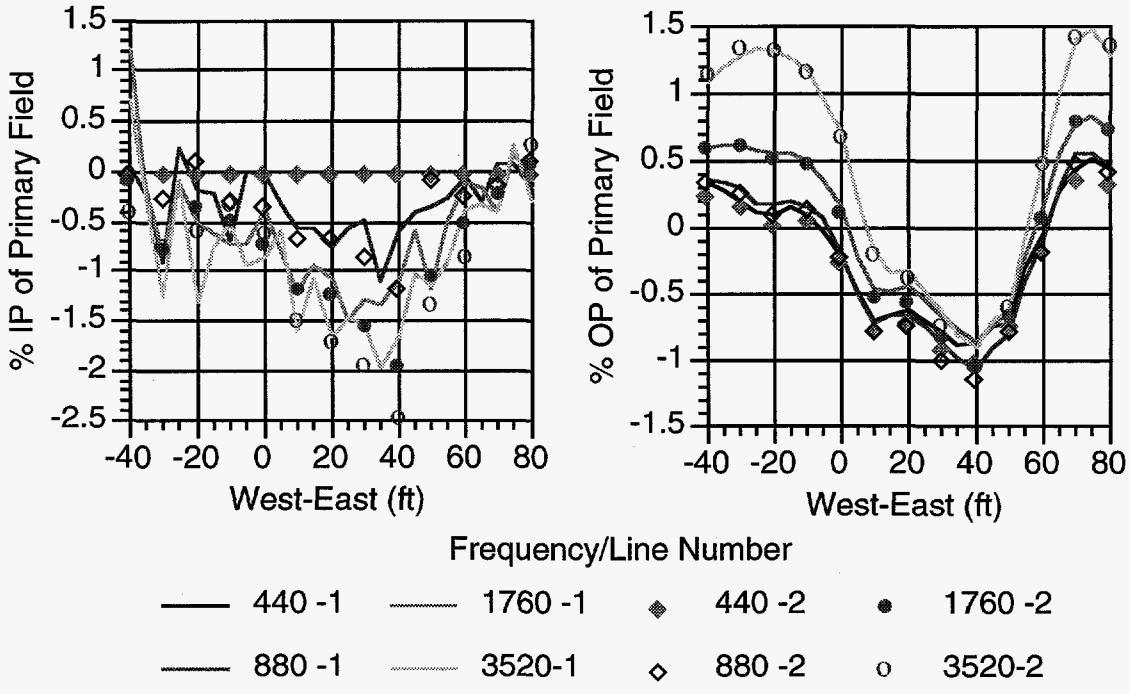

Figure 3 - The repeat measurements along line 7.5N using a 60 foot coil separation. The in-phase component is on the left, and the out-of-phase on the right. Only the four lowest frequencies are shown in order not to clutter the figures.

PRELIMINARY 3-D INVERSION RESULTS

At this point, the images that we are presenting are preliminary in that only two images are available, both of which were produced during the first iteration of the inversion scheme. This is due to the fact that 1) several errors have recently been found both in the original data format as well as recent modifications to the 3D inversion code, 2) for this size problem, using 900 processors of the Intel Paragon at Sandia National Laboratories still takes approximately 5 to 10 hours per iteration depending on the number of source-receiver-frequency combinations that are employed, and 3) the Intel Paragon is highly used and thus at most only three 7 hour runs were obtained each week. Thus progress has been slower than we would have hoped. However even with these setbacks, the results do show some interesting attributes in terms of the data that are needed in order to resolve the target area.

Figure 4 shows an image slice through the center of the pit for a data set consisting only of the 60 foot offset measurements. Notice that the system is detecting the basalt beneath the pit through the fill material. However, also notice that 1) the conductivity that is recovered at the center of the pit (10^{20} S/m) is much higher than we would expect, and 2) the depth to the bottom of the pit (approximately 2 m) is much shallower than the projected depth of 5 to 7 m. We believe that these artifacts may be due to 1) the fact that this is only the first iteration of a very non-linear iterative process, 2) slightly inaccurate forward modeling is corrupting the sensitivity functions (we recently noticed errors in the initial calculations which are most likely the result of the mesh boundaries being too close to the modeling region). On the other hand we believe that the inability to detect a capping layer is a function of the large coil separation versus the relatively thin cap thickness (6 feet) rather than a problem with the inversion. Thus this particular property will probably not change substantially with increasing iterations.

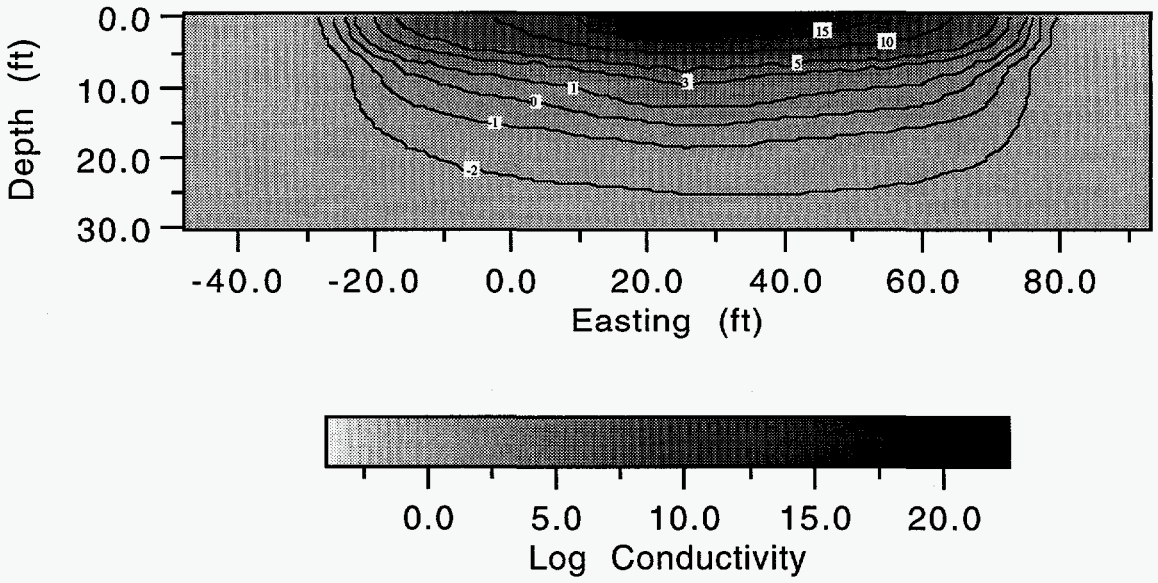

Figure 4 - East-west section of inverted conductivity versus depth along the 0.0N where the inversion scheme has employed eight frequencies and a 60 foot source-receiver separation. These results are for the first iteration of a iterative scheme and are plotted in terms of the log of the conductivity.

To demonstrate what happens if you incorporate multiple offset data into the inversion, in Figure 5 we have plotted the image for the same profile where four frequencies are employed with all three coil separation (only four frequencies were employed due to memory and time limitations). Notice that now we seem to be resolving not only the bottom of the pit, but also the thickness of the capping material. This interpretation, although still crude at this initial stage, seems to illustrate the need for using data that employs multiple source-receiver offsets and frequencies to fully recover the geometry of this type of subsurface structure.

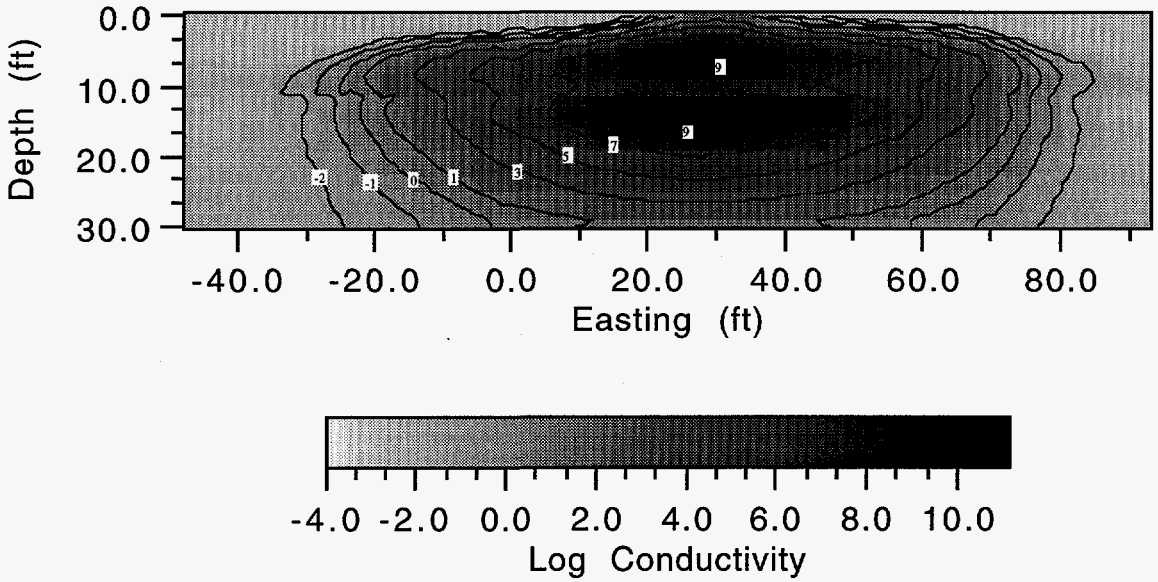

Figure 5 - East-west section of inverted conductivity versus depth along the 0.0N where the inversion scheme has employed four frequencies and 15,30 and 60 foot source-receiver separations. These results are for the first iteration of a iterative scheme and are plotted in terms of the log of the conductivity.

CONCLUSIONS

Although the results presented above are preliminary, they do show hope of recovering the electrical conductivity structure under the four primary lines at the Cold Test Pit. This will allow us to delineate the pit boundaries and depth, although not the pit contents. In addition it appears that more accurate results can be obtained if multiple source-receiver, multiple frequency measurements are combined rather that using only multiple frequencies and a single source separation. However, there is obviously additional work that needs to be done. First of all the non-linear inversion scheme must be allowed to converge, and the forward modeling domain must be redesigned such that the predicted data and sensitivity functions are more accurate. A method of incorporating an upper bound on the conductivity needs to be developed so that values that are unreasonable (i.e. those at the center of the pit) are not allowed to corrupt the solution; we have formulated such a scheme and will be implementing it shortly. A method to determine the accuracy of the images must be constructed. Finally we must touch on the execution time. Although even a super computer such as the Intel Paragon results in execution times that are unreasonable

for the everyday problems that people wish to solve, we believe that for many sites managed by the DOE, DOD, and other branches of government who own these large computers, this type of imaging may be feasible to determine the amount of material that needs to be excavated, and to where and how such excavations should proceed.

ACKNOWLEDGMENTS

This work was performed at Sandia National Laboratories, which is operated for the U.S. Department of Energy. Funding for this project was provided by DOE's office of Basic Energy Sciences, Division of Engineering and Geoscience under contract DE-AC04-94AL85000. The data were collected David Alumbaugh and Louise Pellerin under the VETEM project which was supported by the DOE Office of Technology Development.

REFERENCES

Alumbaugh, D.L., Newman, G.A., Prevost, L., and Shadid, J.N., 1996, Three-dimensional wide band electromagnetic modeling on massively parallel computers: Radio Science , **31**, 1-23.

Apex Parametrics Ltd.,1994, Apex MaxMin I-10 and I-8S EM Systems Operations Manual: Apex Parametrics, Uxbridge, Ontario, Canada.

Constable, S.C., Parker, R.L., and Constable, C.G., 1987, Occam's inversion; a practical algorithm for generating smooth models from electromagnetic sounding data: Geophysics, **52**, 289-300.

Lockheed Idaho Technologies Company (LITCO), 1994, INEL Cold Test Pit: BP-BP726-0394-25M-T, prepared by LITCO for the U.S. Department of Energy Idaho National Engineering Laboratory, Idaho Falls, Idaho.

Mackie, R.L., and Madden, T.R., 1993, Three-dimensional magnetotelluric inversion using conjugate gradients: Geophy. J. Int., **115**, 215-229.

Newman, G.A., and Alumbaugh, D.L., 1997, 3-D massively parallel electromagnetic inversion; part a - theory: Geophy. J. Int., in press for February issue.

Oldenburg, D.W., 1994, Practical strategies for the solution of large-scale electromagnetic inverse problems: Radio Science, **29**, 1081-1099.

Park, S.K., and Van, G.P., 1991, Inversion of pole-pole data for 3-D resistivity structure beneath arrays of electrodes: Geophysics, **56**, 951-960.

Pellerin, L, Alumbaugh, D.L, and Pfeifer, M.C., 1997, The electromagnetic integrated demonstration at the Idaho National Engineering Laboratory Cold Test Pit: Proceedings of SAGEEP '97 (Symposium on the Application of Geophysics to Environmental and Engineering Problems), Reno, Nevada.

Tikhonov, A. N. and Arsenin, V. Y., 1977, Solutions to ill-posed problems: John Wiley and Sons, Inc.

Zhang, J., Mackie, R.L., and Madden, T.R., 1995, Three-dimensional resistivity forward modeling and inversion using conjugate gradients: Geophysics, **60**, 1313-1325.